Biophysical *Journal*
Article

Biophysical Society

Intrinsically Disordered Stress Protein COR15A Resides at the Membrane Surface during Dehydration

Anne Bremer,[1] Ben Kent,[2] Thomas Hauß,[2] Anja Thalhammer,[3] Nageshwar R. Yepuri,[4] Tamim A. Darwish,[4] Christopher J. Garvey,[4] Gary Bryant,[5] and Dirk K. Hincha[1,*]

[1]Max-Planck Institut für Molekulare Pflanzenphysiologie, Potsdam, Germany; [2]Institute for Soft and Functional Materials, Helmholtz-Zentrum Berlin, Berlin, Germany; [3]Physikalische Biochemie, Universität Potsdam, Potsdam, Germany; [4]Bragg Institute, Australian Nuclear Science and Technology Organisation, Lucas Heights, Australia; and [5]Centre for Molecular and Nanoscale Physics, School of Applied Science, RMIT University, Melbourne, Australia

ABSTRACT Plants from temperate climate zones are able to increase their freezing tolerance during exposure to low, above-zero temperatures in a process termed cold acclimation. During this process, several cold-regulated (COR) proteins are accumulated in the cells. One of them is COR15A, a small, intrinsically disordered protein that contributes to leaf freezing tolerance by stabilizing cellular membranes. The isolated protein folds into amphipathic α-helices in response to increased crowding conditions, such as high concentrations of glycerol. Although there is evidence for direct COR15A-membrane interactions, the orientation and depth of protein insertion were unknown. In addition, although folding due to high osmolyte concentrations had been established, the folding response of the protein under conditions of gradual dehydration had not been investigated. Here we show, using Fourier transform infrared spectroscopy, that COR15A starts to fold into α-helices already under mild dehydration conditions (97% relative humidity (RH), corresponding to freezing at -3°C) and that folding gradually increases with decreasing RH. Neutron diffraction experiments at 97 and 75% RH established that the presence of COR15A had no significant influence on the structure of 1-palmitoyl-2-oleoyl-*sn*-glycero-3-phosphocholine (POPC) membranes. However, using deuterated POPC we could clearly establish that COR15A interacts with the membranes and penetrates below the headgroup region into the upper part of the fatty acyl chain region. This localization is in agreement with our hypothesis that COR15A-membrane interaction is at least, in part, driven by a hydrophobic interaction between the lipids and the hydrophobic face of the amphipathic protein α-helix.

INTRODUCTION

Plants are constantly exposed to a multitude of environmental challenges that they cannot evade because of their sessile nature. Consequently, plants have evolved a vast array of physiological adaptations, many of which are triggered in response to particular stimuli. One of the best investigated of these responses is termed cold acclimation (see (1,2) for reviews). It describes the ability of temperate climate plants to increase their freezing tolerance upon exposure to low, but nonfreezing temperatures. Cold acclimation is regulated at the gene expression level, and significant changes in the expression of over 2000 genes have been documented in the model plant, *Arabidopsis thaliana* (e.g., (3,4)). Although elucidating the regulatory networks underlying such expression changes has been a major focus in plant research (see (5,6) for reviews), very little is known about the functional roles that the encoded proteins may play in freezing tolerance.

A group of highly cold-induced genes in *Arabidopsis* has been termed cold-regulated (*COR*) genes (7). Many of the proteins encoded by these genes were later found to be part of the larger group of late embryogenesis abundant (LEA) proteins. LEA proteins are not plant specific, but also occur in many microorganisms and invertebrate animals (8). Their accumulation is almost always induced by cellular dehydration triggered by drought, desiccation, cold, salt, or freezing stress (9). Most LEA proteins are predicted to belong to the group of intrinsically disordered proteins (10). For several LEA proteins, it has been experimentally shown that they are largely unstructured in dilute solutions, but fold into a mainly α-helical structure during drying (see (8,11) for reviews). However, this is not the case for all LEA proteins. In *Arabidopsis*, 51 different LEA proteins have been identified that belong to nine

Submitted March 21, 2017, and accepted for publication June 12, 2017.

*Correspondence: hincha@mpimp-golm.mpg.de

Editor: Jane Dyson.

http://dx.doi.org/10.1016/j.bpj.2017.06.027

different Pfam families that share no sequence similarities (10). Only very few of these proteins have been investigated in detail, making more general structural and functional comparisons impossible.

To-date the best studied COR/LEA protein is COR15A from *A. thaliana*. It is a nuclear-encoded protein that accumulates in the chloroplast stroma during cold acclimation (12–14). The mature protein has a molecular mass of 9 kDa, and is highly hydrophilic with a net charge of −6 at pH 7. COR15A is mainly unstructured in dilute solutions, but folds into amphipathic α-helices in a helix-loop-helix configuration in the presence of high concentrations of glycerol or by complete desiccation (15,16). Folding is further enhanced in the presence of lipid membranes under such conditions of glycerol-induced crowding (17). In vivo, COR15A stabilizes cellular membranes during freezing (16), and in agreement with this finding, the protein also protects liposomes with a lipid composition modeling chloroplast membranes during an in vitro freeze-thaw cycle (16,17). Fourier transform infrared (FTIR) spectroscopy indicates that COR15A forms H-bonds with the sugar headgroup of the chloroplast galactolipid monogalactosyldiacylglycerol in the dry state, and that the protein reduces the phase transition temperature of dried 1-palmitoyl-2-oleoyl-*sn*-glycero-3-phosphocholine (POPC) (15,17). Molecular dynamics simulation and circular dichroism (CD) spectroscopy data suggest that COR15A folds into an amphipathic helix-loop-helix structure in vacuo that is ~85% α-helical (18), and we have hypothesized that the protein interacts with membranes through the hydrophobic face of these helices (17). However, although there is limited experimental evidence for a direct interaction between COR15A and membranes from small- and wide-angle x-ray scattering data (16), experimental information about the orientation and depth of protein penetration is still missing.

In this article, we therefore first determined the extent of the structural transition from unfolded to α-helical in COR15A, along a gradient of relative humidity (RH) from solution to 11% RH, by FTIR spectroscopy. We then used controlled dehydration (97 and 75% RH) to elucidate the position of COR15A in POPC lipid membranes, using neutron diffraction measurements. Our results indicate gradual folding of the protein, with reduced water content and an orientation parallel to the membrane surface at the membrane-water interface, with only shallow penetration into the lipid phase.

MATERIALS AND METHODS

Sample preparation

POPC was purchased from Avanti Polar Lipid (Alabaster, AL). Additionally, chain-deuterated POPC ($POPC^D$) was prepared at the Australian Nuclear Science and Technology Organisation, using a previously published method (19). Chloroform solutions both of POPC or a mixture of $POPC^D$/POPC (10:90 mol/mol) were prepared, dried under a stream of nitrogen, and put under vacuum for at least 12 h to remove traces of solvent. Lipids were rehydrated in double-distilled water, and liposomes were formed using a hand-held extruder with two layers of polycarbonate membranes with 100 nm pores (Avestin, Ottawa, Canada (20)). The plant protein COR15A from *A. thaliana* was expressed and purified as recently described (18). Lyophilized COR15A was rehydrated in double-distilled water and added to the liposome mixture. A 1:10 protein/liposome mass ratio was used for neutron diffraction measurements, and a 1:4 mass ratio was used for FTIR spectroscopy. Samples were pipetted onto either quartz slides (76.2 × 25.4 × 1.0 mm; Alfa Aesar, Ward Hill, MA) for neutron diffraction measurements, or calcium fluoride windows for FTIR spectroscopy. Samples were put under vacuum for at least 12 h, and then rehydrated in chambers of defined RH at 25°C for at least 12 h or at 20°C for 24 h (FTIR). The salt solutions and RHs generated were 97% (potassium sulfate), 93% (potassium nitrate), 85% (potassium chloride), 75% (sodium chloride), 33% (magnesium chloride), and 11% (lithium chloride) (21). Humidity, temperature, and dew point were continuously recorded using EL-USB-2 Temperature and Humidity Data Loggers from Lascar Electronics (Whiteparish, UK).

Neutron diffraction measurements and data analysis

A membrane sample consisting of a stack of lipid bilayers is a quasi, one-dimensional crystal, and the structure of a membrane along its profile perpendicular to the membrane plane can be determined by diffraction experiments using x rays or neutrons. As a result of such experiments, the scattering length density (SLD) is determined along the profile axis. In the case of x rays, the scattering length of an atom is determined by the number of its electrons and increases with the atomic number Z, whereas the scattering length for neutrons is determined by its nucleus and appears randomly by element or isotope. In the case of a neutron diffraction measurement, the coherent scattering length b_c determines the SLD profile, and the fact that the isotopes of hydrogen ^1H (H, protium) and ^2H (D, deuterium) have vastly different scattering lengths, with $b_c(H) = -3.739$ fm and $b_c(D) = 6.671$ fm (22), is often exploited as contrast variation or isotopic replacement in neutron diffraction experiments.

Neutron membrane diffraction was performed on the V1 membrane diffractometer at the Helmholtz-Zentrum Berlin (Berlin, Germany). The wavelength of the neutron beam was 4.56 Å. An area detector (19 × 19 cm) was rotated around the sample at a constant distance of 1.0 m to define the scattering angle θ. The sample on a quartz slide was mounted vertically and sealed in an aluminum container of a defined RH and temperature. Humidity was set at 97 or 75% using saturated salt solutions, whereas temperature was fixed at 25 ± 0.1°C, using a JULABO temperature controller to circulate water through tubing surrounding the container.

Well-ordered multilamellar lipid stacks give rise to intensity peaks caused by the constructive interference of scattered neutrons in neutron diffraction measurements. Thereby, the distance (d) of adjacent membranes is described by the Bragg equation

$$2d \sin\theta = h\lambda, \quad (1)$$

where θ is half of the scattering angle 2θ, i.e., the angular position of the peaks, h is the diffraction order, and λ is the wavelength of the neutron beam. SLD profiles of the samples were reconstructed using Fourier synthesis (23). In all measurements, no Bragg peaks higher than the fifth order were detected, and rocking curve measurements were performed for each of the first five diffraction orders. A single rocking curve measurement consisted of fixing the detector at the 2θ position of the diffracted peak, and rotating the sample through a small angle relative to the incident beam. The recorded intensities for each angle θ were then summed to produce the final rocking curve. These were fit with a Gaussian function and the area of the curve used to determine the intensity of each peak. These intensities were corrected for the different pathlengths of the scattered neutrons through the sample at different scattering angles, using

absorption and Lorentz corrections to obtain the structure factor magnitudes *f(h)* (24),

$$f(h) = \sqrt{I(h)\,A(h)\,\sin\theta}, \quad (2)$$

where *I(h)* is the scattered intensity, *A(h)* is the absorption correction, and $\sin\theta$ is the Lorentz correction.

The SLD in real space across the unit cell of a single bilayer and water layer is related to the full structure factor by a Fourier transformation. The structure factors *f(h)* sample the full structure factor at discrete points. A real-space SLD profile *ρ(z)* can then be synthesized by a Fourier cosine series,

$$\rho^*(z) = \rho_0^* + \frac{2}{dk}\sum_{h=1}^{n} f(h)\left(\cos\frac{2\pi hz}{d}\right), \quad (3)$$

where *d* is the repeat spacing (d-spacing), *k* is an instrumental scaling constant, ρ_0 is the average scattering density of the unit cell, and *z* is the distance from the center of the bilayer.

The SLD profiles were scaled to a "per lipid" absolute scale by first calculating the average SLD ρ_0 from the scattering lengths of the constituents of the unit cell. This shifts the profiles to fluctuations around the expected average SLD of the measured unit cell. The instrumental scaling constants *(k)*, which are generally unknown and depend on each individual measurement condition and sample, were then determined by using the variation of the water layer after measurements from the three water contrasts. Variation of the water-layer contrast has no effect on the regions of the SLD profiles that are not penetrated by water molecules, (i.e., the center of the bilayer). The scaling constants were varied so that differences in the water-free sections of the profiles between separate water contrast measurements of each sample were minimized.

The spatial resolution of the SLD profiles depends on the number of terms in the measured reflections. A finite number of terms leads to Fourier truncation artifacts in the profiles. The artifacts most commonly show up as overshoots or small ripples in regions of high SLD variation. In all systems measured in this study, five reflections were routinely measured. Uncertainty of the SLD profiles was calculated using the equation from Dante *et al.* (25).

FTIR spectroscopy

Solutions containing COR15A, COR15A, and POPC, or only POPC liposomes were spread on calcium fluoride windows and equilibrated at different RH levels as described above. Additionally, anhydrous samples under vacuum and samples rehydrated over heavy water were prepared. A second calcium fluoride window was placed on top of the sample to avoid rehydration. FTIR spectra were recorded from 4000 to 900 cm^{-1} with a PerkinElmer (Rodgau, Germany) GX2000 FTIR spectrometer. Sixteen spectra were coadded and analyzed using the Spectrum 10.4.3 software (PerkinElmer). At least three samples per condition were measured.

RESULTS

COR15A gradually folds upon dehydration

Gradual folding of COR15A in the presence of increasing concentrations of glycerol has been shown previously (18). In addition, we provided evidence that partial folding in the presence of glycerol is necessary for protein interactions with POPC membranes (16,17). However, whether reduced water activity due to reduced RH would also induce folding was not known. Therefore, before performing neutron diffraction experiments at different RHs, we investigated whether these conditions would induce folding in COR15A. The secondary structure of the protein was assessed by FTIR spectroscopy in response to RH between 97 and 11%. The Amide I peak of the FTIR spectrum contains information about protein secondary structure. It is the sum of several underlying peaks that are indicative of different secondary structure elements, such as α-helices (1660–1650 cm^{-1}), β-sheet (1640–1620 cm^{-1}), and unordered regions (1650–1640 cm^{-1}) (26,27). Because water absorbs strongly in the FTIR spectral region where the Amide I peak is localized, such structural studies in solution are usually performed in heavy water to shift the water peak away from the Amide I peak (27,28). To control for the contribution of the water peak to the Amide I peak, we measured FTIR spectra at all RH levels for POPC liposomes in the absence of protein, and normalized the spectra to the lipid C=O peak (Fig. S1). The data showed that even at 97% RH, the highest RH used in our experiments, the water peak was very small compared to the Amide I peak in samples containing liposomes and COR15A. Consequently, subtracting the water peak from the Amide I peak did not result in significant changes in Amide I peak positions.

Under conditions of high humidity and in solution (heavy water), COR15A showed a peak at ~1644 cm^{-1} (Fig. 1, *A* and *C*), indicating the presence of mainly unordered regions, in agreement with previous CD spectroscopy experiments (15). Upon dehydration, the Amide I peak was shifted toward higher wavenumbers up to ~1655 cm^{-1}, indicating a predominantly α-helical structure in dehydrated and anhydrous COR15A, again in agreement with previous CD measurements (15) and molecular dynamics simulations (18). The presence of POPC liposomes had no significant influence on the Amide I peak position at any of the investigated RHs (Fig. 1, *B* and *C*).

COR15A is located near the headgroup region of POPC lipids in dehydrated samples

We probed the location of COR15A molecules relative to the bilayer membrane, using neutron membrane diffraction. Aligned systems of pure POPC and POPC/COR15A at a 10:1 mass ratio were used to reconstruct total average SLD profiles across the bilayers. In addition, measurements were performed with $POPC^D$ using a 10:90 $POPC^D$/POPC molar ratio. Typical diffraction peaks for POPC ± COR15A at 97% RH are shown in Fig. 2. The diffraction peaks were Gaussian in shape. They were shifted slightly to smaller angles in the presence of COR15A because of an increase of 1–2 Å in the repeat spacing of the bilayer system (Fig. 3). This increase was within the estimated errors. However, it was consistent for all samples at both RHs.

Since COR15A is localized in chloroplasts and chloroplast membranes do not contain phosphatidylcholine, we also performed neutron diffraction measurements with membranes

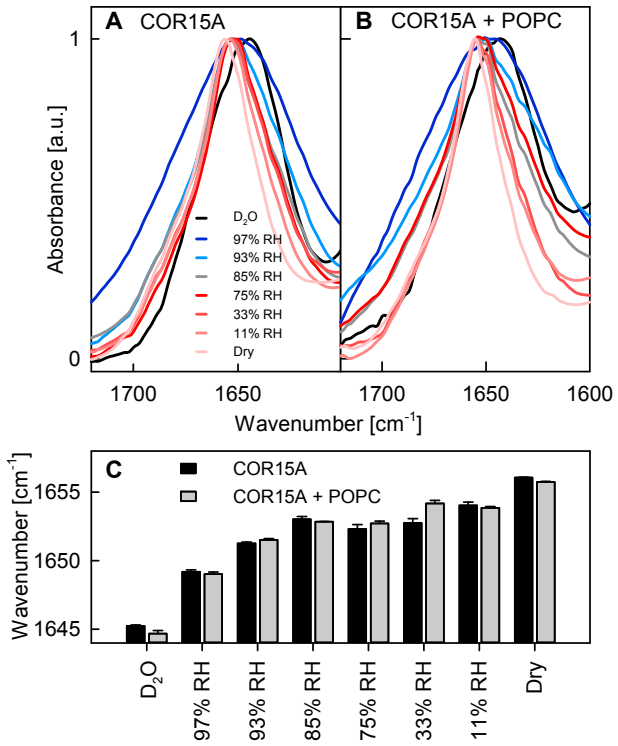

FIGURE 1 Amide I peak of COR15A without (*A*) or with (*B*) POPC membranes at different RHs. Because the OH absorbance peak of water overlaps with the Amide I peak of the proteins, the water band of FTIR spectra from samples containing only POPC was subtracted from the spectra of the protein at the respective RH (see Material and Methods for more information). The Amide I peak positions ± mean ± SE ($n = 3$) are shown in (*C*). POPC liposomes were present at a 1:4 protein/lipid mass ratio.

containing chloroplast glycolipids. Unfortunately, however, these measurements only yielded one diffraction peak and were therefore not suitable for SLD reconstruction. Structure factors were obtained using Eq. 2 in Materials and Methods.

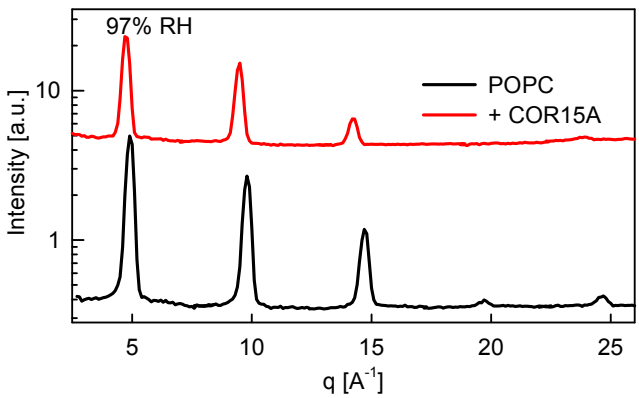

FIGURE 2 Neutron membrane diffraction results, showing the measured peaks for POPC and POPC ± COR15A equilibrated at 97% RH, with a 0.08 heavy water volume fraction in water. Each peak is fit with a Gaussian function to determine the scattered intensity and position. The baseline is determined by the incoherent scattering of the samples and vertically offset for clarity.

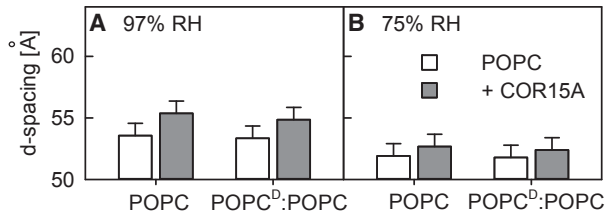

FIGURE 3 Bilayer repeat spacing, referred to as d-spacing, determined by neutron diffraction measurements of nondeuterated POPC and a 10:90 $POPC^D$/POPC mixture in the absence and presence of COR15A equilibrated at 97 (*A*) and 75% RH (*B*).

Each structure factor $f(h)$ for a centro-symmetric system, such as an aligned bilayer system, can be either positive or negative. To determine these phases, we used an isomorphous replacement method. This was achieved by measuring each sample three times, after equilibration with saturated salt solutions containing 8, 20, or 50% heavy water in water (see (29) for more information on structure factor phasing). Each increase in the heavy water content of the water phase increases the SLD of the water layer. In Fourier space, this either increases the magnitude of a structure factor or decreases it depending on the phase of the structure factor. The sign of each structure factor is thus chosen according to the sign of the gradient of the structure factor as a function of heavy water volume fraction. Correctly phased structure factors will then exhibit a linear relationship with the volume fraction of heavy water, as shown in Fig. 4. For consistency, all profiles are shown for 8% heavy water, where the SLD of the water layer equals zero.

Neutron SLD profiles of POPC ± COR15A were reconstructed using Fourier synthesis. The profiles represent one lipid bilayer together with its hydration shell (Fig. 5). The profiles are shown so that $z = 0$ Å is the bilayer center, where the methyl groups are located. Moving away from the center of the bilayer, the conformation of the partially saturated POPC hydrocarbon chains results in plateaus at around $|6|$ Å (30). Further out from the center of the bilayer, the glycerol backbone and the polar lipid headgroup give rise to the main peaks at $|17|$ Å in the SLD profile because of their high positive scattering lengths. The 95% confidence limits shown were calculated from the errors in the structure factor magnitudes.

The presence of COR15A had little effect on the overall structure of the bilayer. It retained the same qualitative profile when the protein was added to the system. However, there was an increased scattering density in the backbone and headgroup parts of the membrane, as well as in the water layer. This increase was well outside the 95% confidence band, whereas the center of the bilayer in the hydrocarbon chain region remained unchanged within the error margin when COR15A was added. The differences in the SLD profiles at around $|10|$ Å may be attributed to a slight increase in the width of the headgroup region in the presence of COR15A, caused by intercalation of the protein.

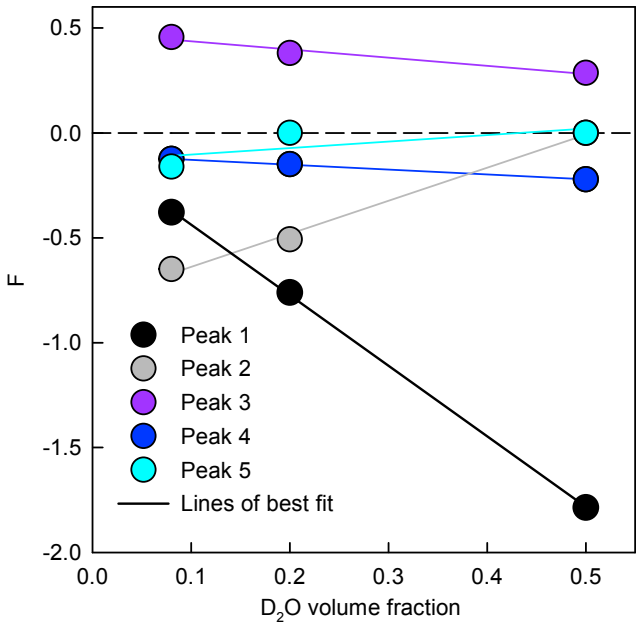

FIGURE 4 Phasing of 10:90 POPC^{D}/POPC at 97% RH for three different heavy water volume fractions. The phase of each structure factor is chosen according to the sign of the gradient of the intensity variation as a function of heavy water volume fraction (volume fractions of 0.08, 0.2, and 0.5). The correctly signed structure factors then show a linear relationship with the heavy water volume fraction, as shown here.

The SLD of COR15A at the concentrations used in this study was quite low. This complicates the determination of the contribution of the protein and the scaling of the profiles. This is particularly noticeable in the difference profiles, which are susceptible to Fourier truncation artifacts in the two contributing profiles. Therefore, we performed neutron diffraction measurements of POPC with deuterated hydrocarbon tails (POPC^{D}), using a 10:90 POPC^{D}/POPC molar ratio. This has the advantage of modulating the SLD of the POPC profile while leaving the contribution of the protein constant, thus allowing verification of the scaling procedure, as well as producing COR15A difference profiles to compare with the POPC system (Fig. 6). The results from both systems were consistent.

To determine the changes induced by the presence of COR15A, the pure POPC system profiles were subtracted from the POPC ± COR15A and POPC^{D}/POPC ± COR15A profiles to create difference profiles (Fig. 6). Although subtracting the pure POPC profiles highlights the effects of COR15A, the difference profiles are more susceptible to Fourier truncation artifacts and the slight increase in headgroup width due to the presence of the protein. This can be observed in the higher spatial frequency ripples of the difference profiles and the discrepancies between the POPC and POPC^{D}/POPC systems. Nevertheless, there is a clear confinement of COR15A to the water layer and outer section of the bilayer in both systems and at both humidities.

The SLD profiles are a time-averaged description of the SLD per unit length across the unit cell. The profiles can be decomposed into quasimolecular segments, each with a known SLD calculated from the coherent scattering lengths of the constituent atoms. These contributions are usually

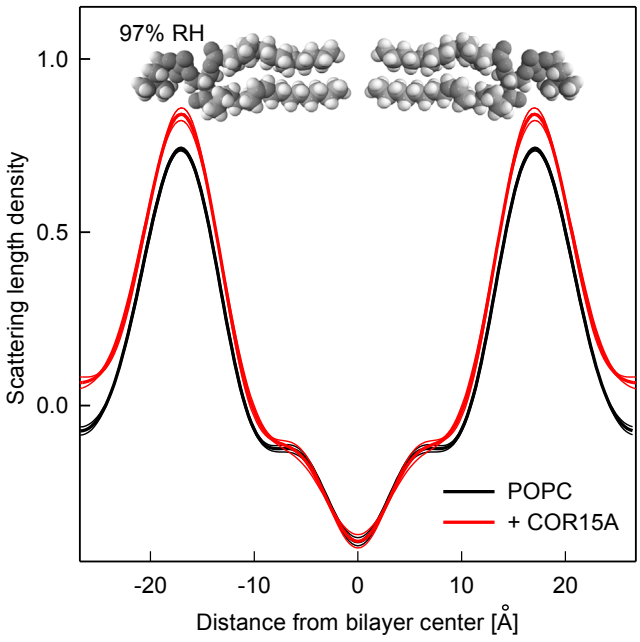

FIGURE 5 Bilayer centered SLD profiles from neutron diffraction measurements of POPC ± COR15A equilibrated at 97% RH. A 1:10 protein/lipid mass ratio was used. 95% confidence limits are shown. The schematic of the lipids is a guide to the eye and indicates the average lipid position, as indicated by the SLD.

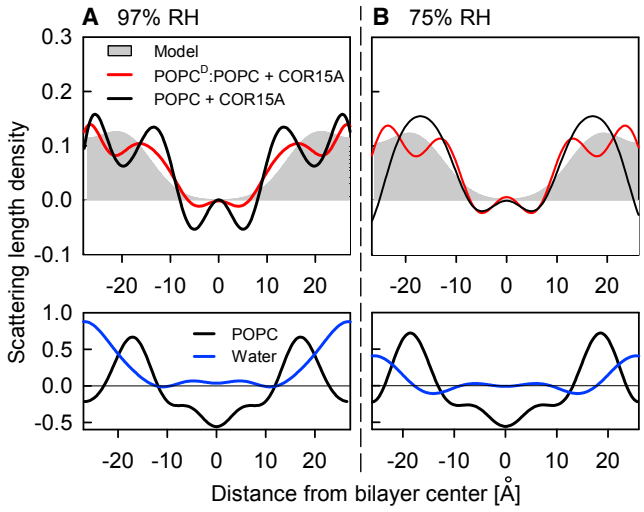

FIGURE 6 SLD difference profiles showing the distribution of COR15A in the POPC bilayer system at RHs of 97 (*A*) and 75% (*B*). Difference profiles (*top*) were generated by subtracting the POPC profile from the profile of POPC ± COR15A. The gray area shows the calculated SLD profile of COR15A, determined using a Gaussian distribution function for the protein. The bottom panels show the profiles of the POPC bilayer together with the water distribution, calculated as the difference between SLD profiles measured at volume fractions of 0.5 and 0.08 heavy water.

described by a Gaussian function because of the fluid motion of the systems studied (31,32). For a bilayer system, this decomposition is difficult without a satisfactory initial guess of each of the overlapping segmental contributions. In this case, we simply model the contribution of the COR15A molecule using a single Gaussian distribution. This contribution can be directly compared with the difference profiles defined above (Fig. 6). The area under the curve of the calculated Gaussian function is equal to the calculated total scattering length of COR15A in the bilayer system. This is simply the sum of the coherent scattering lengths of the atoms comprising COR15A, multiplied by the COR15A/lipid molar ratio. This scattering length value (1.78×10^{-14} m) is fixed as the area under the curve, whereas the width and amplitude of the distribution are allowed to vary so that the difference between the calculated SLD profile and the difference profile is minimized.

The profiles show that the time-averaged distribution of COR15A extends as far as the first five to six carbon atoms of the acyl chains. The COR15A molecule is therefore capable of inserting between the glycerol backbone and headgroups of the lipid molecules in this system. This is further into the bilayer than the water molecules penetrate, and indicates that the protein is not simply a freely dissolved solute in the water phase, but directly interacting with the lipid phase.

DISCUSSION

COR15A is accumulated in the chloroplasts of *Arabidopsis* leaves when the plants are exposed to low temperatures (12–14). This accumulation is necessary for the plants to obtain their full, cold-acclimated freezing tolerance (16). Although it is clear from our previous work that COR15A is able to protect membranes from damage during freezing and thawing (16,17), it was still unresolved how this highly hydrophilic, intrinsically disordered protein may interact with membranes to achieve this effect. In plant leaves, where COR15A is accumulated in the cold, ice crystallization occurs in the intercellular spaces, leading to vapor-phase dehydration of the cells. This freeze-induced dehydration leads to an increase in intracellular solute concentrations and to membrane destabilization (33). We hypothesized earlier that partial folding of the protein into amphipathic α-helices because of this freeze-induced increase in crowding may generate a hydrophobic face on the protein that could be responsible for a protective protein-membrane interaction (17).

Here, we have shown that already mild dehydration at 97% RH, which corresponds to −4 MPa or freezing to −3°C (34), is sufficient to induce partial folding in COR15A. Since cold-acclimated *Arabidopsis* leaves can survive freezing to temperatures well below −10°C (35), this indicates that this folding reaction takes place under physiologically relevant conditions. Interestingly, we did not observe an additional increase in folding during dehydration in the presence of membranes by FTIR spectroscopy, although a small increase was apparent from CD spectroscopy experiments (16,17) in the presence of high concentrations of glycerol ($\geq$50 vol%). This may reflect slightly different folding behavior of COR15A in the two experimental systems, but it should also be noted that in general, CD spectroscopy is more sensitive for the detection of α-helical structure than FTIR (36).

Although COR15A is localized in chloroplasts, and therefore its natural target membranes do not contain phosphatidylcholine, our data still reveal the general mode of interaction of this amphipathic helical protein with lipid bilayers. Similarly, our earlier small- and wide-angle x-ray scattering data indicate that COR15A interacts with membranes, and that POPC bilayer thickness is slightly reduced in the presence of COR15A and 50% glycerol, whereas interlipid chain distance is increased (16). Further, x-ray scattering and NMR experiments show a stabilization of the lamellar lipid phase in lipid mixtures containing nonbilayer lipids (37). Together with the fact that COR15A is able to protect liposomes from leakage of soluble content during a freeze-thaw cycle (16,17), these data suggest a direct interaction of COR15A with membranes under conditions of partial dehydration. However, it was unclear from these data how the COR15 molecule is oriented relative to the bilayer surface, and whether it interacts with the hydrophobic fatty acyl chains of the lipids or only with the hydrophilic headgroups. Since COR15A is a highly hydrophilic protein that folds into amphipathic α-helices during dehydration (18), both depths of insertion seemed physically possible.

The substrate-supported oriented POPC bilayers studied here provide a simple model of the stacking and close approach that cellular membranes may undergo upon dehydration, e.g., during extracellular freezing. The RHs of 97 and 75% RH used in this study are equivalent to equilibrium freezing to −3 and −33°C, respectively (34). These temperatures are well in the range of freezing temperatures that herbaceous plants may encounter and survive in temperate climate regions of the Earth (see (33) for a review).

Our data provide clear evidence that, under dehydration conditions, COR15A partially folds and inserts into the membrane parallel to the surface. The neutron diffraction results indicate changes in the SLD in the membrane headgroup region when COR15A is added to the system. These density profiles contain contributions from the SLD of COR15A, as well as changes to the POPC SLD profile due to the presence of COR15A. By making the assumption that only insignificant perturbations are made to the POPC profile, the difference profiles can be treated as SLD profiles of the COR15A molecule, showing the location of the protein in relation to the bilayer. Although the experimental difference profiles are more complex than a simple Gaussian profile, the areas under the curves are similar to those under the Gaussian model curves, indicating that the assumption that the lipid

profile is not significantly disturbed by the presence of the protein is valid, and difference profiles are related to the density profiles of COR15A. The more complex distribution profiles of the protein in the bilayer system most likely result from the limited resolution of the membrane diffraction measurements due to the relatively low contrast of the COR15A molecule. This makes Fourier truncation artifacts a likely cause for the non-Gaussian difference profiles.

However, it is clear from these profiles that COR15A locates in the headgroup region of the POPC bilayer at both humidities. The center of the bilayer remains protein free, as would be expected for a hydrophilic, highly charged protein without a transmembrane segment. Consequently, the structure of the POPC bilayer is not significantly affected by the presence of the protein. A small change in the bilayer thickness could contribute to the small increase in the repeat spacing. Determining the position of the POPC headgroup precisely enough in the presence of COR15A to evaluate such a change in bilayer thickness is not trivial, because of the requirement to deconvolve the headgroup profile and the COR15A profile. However, the similarity in the hydrocarbon tail region of the POPC bilayer in the absence and presence of protein suggest very little changes in the bilayer dimensions. Therefore, the increase in d-spacing is most likely because of the presence of the protein in the interbilayer solution and the headgroup region, thereby increasing its volume.

Although COR15A molecules are present in the aqueous space between the membranes, they also penetrate the membrane surface further into the bilayer than the water molecules, reaching as far as the first five to six methylene groups of the fatty acyl chains. This location is in agreement with our hypothesis that the hydrophobic face of the amphipathic α-helices of the protein is important for the observed effects of the protein on membranes. Such a localization is not common of all membrane cryoprotectants. Cryoprotective sugars, such as trehalose, do not interact with membranes under similar conditions, but rather are confined to the aqueous space between the membrane stacks (29,38).

CONCLUSION

Our study shows that the highly hydrophilic, intrinsically disordered plant stress protein COR15A folds into α-helices upon mild dehydration. Under the same conditions, the protein localizes to the membrane-water interphase, penetrating the membrane to the level of the first methylene groups of the fatty acyl chains. Further research is required to show how the protein interacts with membranes containing chloroplast galactolipids, and how such interactions result in membrane stabilization during freezing and thawing.

SUPPORTING MATERIAL

One figure is available at http://www.biophysj.org/biophysj/supplemental/S0006-3495(17)30677-X.

AUTHOR CONTRIBUTIONS

A.B., B.K., A.T., G.B., and D.K.H. conceived the project and all authors participated in the experimental design and development of experimental strategies. A.B. performed the FTIR measurements and A.B. and D.K.H. performed the FTIR data analysis. A.B., B.K., and T.H. performed the neutron diffraction experiments and data analysis. N.R.Y., T.A.D., and C.J.G. contributed important reagents. A.B., B.K., and D.K.H. wrote the manuscript with input from all authors.

ACKNOWLEDGMENTS

We thank the Helmholtz-Zentrum Berlin for providing beam time on the Membrane Diffractometer V1 and Werner Graf for technical assistance. A.B. gratefully acknowledges a PhD fellowship from the University of Potsdam. A.T. gratefully acknowledges support from Prof. Robert Seckler (University of Potsdam).

This research was supported by funds from the Max-Planck Society.

REFERENCES

1. Preston, J. C., and S. R. Sandve. 2013. Adaptation to seasonality and the winter freeze. *Front. Plant Sci.* 4:167.
2. Xin, Z., and J. Browse. 2000. Cold comfort farm: the acclimation of plants to freezing temperatures. *Plant Cell Environ.* 23:893–902.
3. Hannah, M. A., A. G. Heyer, and D. K. Hincha. 2005. A global survey of gene regulation during cold acclimation in *Arabidopsis thaliana*. *PLoS Genet.* 1:e26.
4. Hannah, M. A., D. Wiese, …, D. K. Hincha. 2006. Natural genetic variation of freezing tolerance in Arabidopsis. *Plant Physiol.* 142:98–112.
5. Shinozaki, K., K. Yamaguchi-Shinozaki, and M. Seki. 2003. Regulatory network of gene expression in the drought and cold stress responses. *Curr. Opin. Plant Biol.* 6:410–417.
6. Thomashow, M. F. 2010. Molecular basis of plant cold acclimation: insights gained from studying the CBF cold response pathway. *Plant Physiol.* 154:571–577.
7. Thomashow, M. F. 1999. Plant cold acclimation: freezing tolerance genes and regulatory mechanisms. *Annu. Rev. Plant Physiol. Plant Mol. Biol.* 50:571–599.
8. Hand, S. C., M. A. Menze, …, D. Moore. 2011. LEA proteins during water stress: not just for plants anymore. *Annu. Rev. Physiol.* 73:115–134.
9. Tunnacliffe, A., D. K. Hincha, …, D. Macherel. 2010. LEA Proteins: versatility of form and function. *In* Dormancy and Resistance in Harsh Environments. E. Lubzens, J. Cerda, and M. Clark, editors. Springer, Berlin, pp. 91–108.
10. Hundertmark, M., and D. K. Hincha. 2008. LEA (late embryogenesis abundant) proteins and their encoding genes in *Arabidopsis thaliana*. *BMC Genomics.* 9:118.
11. Hincha, D. K., and A. Thalhammer. 2012. LEA proteins: IDPs with versatile functions in cellular dehydration tolerance. *Biochem. Soc. Trans.* 40:1000–1003.
12. Nakayama, K., K. Okawa, …, T. Inaba. 2007. Arabidopsis Cor15am is a chloroplast stromal protein that has cryoprotective activity and forms oligomers. *Plant Physiol.* 144:513–523.
13. Candat, A., P. Poupart, …, D. Macherel. 2013. Experimental determination of organelle targeting-peptide cleavage sites using transient expression of green fluorescent protein translational fusions. *Anal. Biochem.* 434:44–51.
14. Lin, C., and M. F. Thomashow. 1992. DNA-sequence analysis of a complementary-DNA for cold-regulated Arabidopsis gene COR15 and characterization of the COR15 polypeptide. *Plant Physiol.* 99:519–525.

15. Thalhammer, A., M. Hundertmark, …, D. K. Hincha. 2010. Interaction of two intrinsically disordered plant stress proteins (COR15A and COR15B) with lipid membranes in the dry state. *Biochim. Biophys. Acta.* 1798:1812–1820.

16. Thalhammer, A., G. Bryant, …, D. K. Hincha. 2014. Disordered cold regulated15 proteins protect chloroplast membranes during freezing through binding and folding, but do not stabilize chloroplast enzymes in vivo. *Plant Physiol.* 166:190–201.

17. Bremer, A., M. Wolff, …, D. K. Hincha. 2017. Folding of intrinsically disordered plant LEA proteins is driven by glycerol-induced crowding and the presence of membranes. *FEBS J.* 284:919–936.

18. Navarro-Retamal, C., A. Bremer, …, A. Thalhammer. 2016. Molecular dynamics simulations and CD spectroscopy reveal hydration-induced unfolding of the intrinsically disordered LEA proteins COR15A and COR15B from *Arabidopsis thaliana*. *Phys. Chem. Chem. Phys.* 18:25806–25816.

19. Yepuri, N. R., T. A. Darwish, …, P. J. Holden. 2016. Synthesis of per-deuterated 1-palmitoyl-2-oleoyl-sn-glycero-3-phosphocholine ([D82] POPC) and characterization of its lipid bilayer membrane structure by neutron reflectometry. *Chempluschem.* 81:315–321.

20. MacDonald, R. C., R. I. MacDonald, …, L. R. Hu. 1991. Small-volume extrusion apparatus for preparation of large, unilamellar vesicles. *Biochim. Biophys. Acta.* 1061:297–303.

21. Greenspan, L. 1977. Humidity fixed points of binary saturated aqueous solutions. *J. Res. Natl. Bur. Stand.* 81A:89–96.

22. Sears, V. F. 1992. Neutron scattering lengths and cross sections. *Neutron News.* 3:26–37.

23. Worcester, D. L. 1976. Neutron diffraction studies of biological membranes and membrane components. *Brookhaven Symp. Biol.* 27:III37–III57.

24. Franks, N. P., and W. R. Lieb. 1979. The structure of lipid bilayers and the effects of general anaesthetics. an x-ray and neutron diffraction study. *J. Mol. Biol.* 133:469–500.

25. Dante, S., T. Hauss, and N. A. Dencher. 2002. Beta-amyloid 25 to 35 is intercalated in anionic and zwitterionic lipid membranes to different extents. *Biophys. J.* 83:2610–2616.

26. Byler, D. M., H. Susi, and H. M. Farrell, Jr. 1983. Laser-Raman spectra, sulfhydryl groups, and conformation of the cystine linkages of beta-lactoglobulin. *Biopolymers.* 22:2507–2511.

27. Barth, A. 2007. Infrared spectroscopy of proteins. *Biochim. Biophys. Acta.* 1767:1073–1101.

28. Susi, H., and D. M. Byler. 1986. Resolution-enhanced fourier transform infrared spectroscopy of enzymes. *Methods Enzymol.* 130:290–311.

29. Kent, B., T. Hauß, …, C. J. Garvey. 2015. Direct comparison of disaccharide interaction with lipid membranes at reduced hydrations. *Langmuir.* 31:9134–9141.

30. Büldt, G., H. U. Gally, …, G. Zaccai. 1979. Neutron diffraction studies on phosphatidylcholine model membranes. I. Head group conformation. *J. Mol. Biol.* 134:673–691.

31. Hristova, K., C. E. Dempsey, and S. H. White. 2001. Structure, location, and lipid perturbations of melittin at the membrane interface. *Biophys. J.* 80:801–811.

32. Wiener, M. C., and S. H. White. 1992. Structure of a fluid dioleoylphosphatidylcholine bilayer determined by joint refinement of x-ray and neutron diffraction data. III. Complete structure. *Biophys. J.* 61:434–447.

33. Steponkus, P. L. 1984. Role of the plasma-membrane in freezing-injury and cold-acclimation. *Annu. Rev. Plant Physiol.* 35:543–584.

34. Bryant, G., and K. L. Koster. 2004. Dehydration of solute-lipid systems: hydration forces analysis. *Colloids Surf. B Biointerfaces.* 35:73–79.

35. Zuther, E., E. Schulz, …, D. K. Hincha. 2012. Clinal variation in the non-acclimated and cold-acclimated freezing tolerance of *Arabidopsis thaliana* accessions. *Plant Cell Environ.* 35:1860–1878.

36. Pribić, R., I. H. van Stokkum, …, M. Bloemendal. 1993. Protein secondary structure from Fourier transform infrared and/or circular dichroism spectra. *Anal. Biochem.* 214:366–378.

37. Steponkus, P. L., M. Uemura, …, M. F. Thomashow. 1998. Mode of action of the COR15a gene on the freezing tolerance of *Arabidopsis thaliana*. *Proc. Natl. Acad. Sci. USA.* 95:14570–14575.

38. Lenné, T., C. J. Garvey, …, G. Bryant. 2009. Effects of sugars on lipid bilayers during dehydration–SAXS/WAXS measurements and quantitative model. *J. Phys. Chem. B.* 113:2486–2491.